JOURNAL OF CATALYSIS **176,** 52–60 (1998)
ARTICLE NO. CA982002

DRIFTS Studies of Surface Properties of Steamed FCC Catalysts

Xinsheng Liu,[1] Ralph E. Truitt, and Gail D. Hodge

Engelhard Corporation, Research Center, 101 Wood Avenue, Iselin, New Jersey 08820

Received March 31, 1997; revised December 31, 1997; accepted January 5, 1998

Surface changes of pure zeolites HY and FCC catalysts after calcination and steaming were studied using the conventional pyridine adsorption-DRIFTS method. The results show that (1) some adsorbed pyridine concomitantly interacts with acid sites (Lewis) and their adjacent Si–OH groups; (2) Si–OH–Al Brönsted acid sites in small cages are easier to be destroyed by steaming than those in supercages; (3) steaming produces new types of Brönsted acid sites in zeolites and FCC catalysts. Species with different origins may have similar IR absorption; (4) the new type of acid sites produced in FCC catalysts at later stages of steaming dominate catalytic cracking activity; and (5) the newly–formed Brönsted acid sites have lower acid strength than the original ones in the zeolites.

© **1998 Academic Press**

INTRODUCTION

Steaming is one of the most important processes in the preparation and during the use of fluid cracking catalysts (FCC). Many studies have concentrated on the surface acidity and structural changes of zeolites from this process (1–6). This information is essential for understanding the mechanisms of acid-catalyzed reactions. Steaming causes dealumination, acidity adjustment, and generation of strong acid sites in zeolites (4–6). Ino *et al.* (6) very recently correlated the structures of FCC catalysts under various calcination and steaming conditions with their catalytic performance. They proposed that framework 0-NNN Al sites (no Al in its next nearest neighbor) control zeolite cracking activity, while the other types of framework Al (1,2,3,4-NNN Al) contribute to coking. Even though the nature of active sites in FCC catalysts is better understood in recent years, details about how the structure and surface acidity change upon calcination and steaming are still unavailable. In the present study, we concentrate on the structures and surface acidity of commercial FCC catalysts upon steaming using the conventional pyridine-IR spectroscopic method (7–8), and try to answer the following questions:

1. How does the acidity change upon steaming?
2. Do the different types of acidic OH groups change all in the same way upon steaming?
3. Does the steaming create any new type of Brönsted acid catalytic sites?

EXPERIMENTAL

Chemicals, Zeolites and FCC Catalysts

Pyridine was purchased from Aldrich and transferred from a newly opened bottle to a stainless steel bottle on the automation line in a dry box under flowing dry N_2. NH_4Y (LZ62, Si/Al = 2.5, Na_2O, 2.5% by weight) was also purchased from Aldrich and calcined under so-called shallow-bed and deep-bed calcination conditions (9). The steamed HY sample (Si/Al = 9.2, Na_2O, 0.18% by weight) was kindly provided by Dr. D. Harris in Engelhard Corporation and was made by steaming NH_4Y at 730°C under 100% humidity. The USY based FCC catalysts were made via an *in situ* zeolite crystallization (10). Kaolin microspheres were first calcined at 950°C, then aged in sodium hydroxide for 6 h at 37°C, followed by zeolite crystallization at 82°C. The microspheres containing ~40 wt% zeolites (the rest being amorphous clay left over (matrix) from the crystallization) were subsequently ion-exchanged to a level of 1 wt% rare earth metal ions, with the remaining charge balancing ions being ammonium (Na_2O, <0.3% by weight). Steaming of the samples was carried out at two temperatures, 775°C and 815°C, with 100% humidity for 24 h, during which samples were taken at different time intervals.

Instruments and Procedures for Acidity Measurements

Diffuse reflectance Fourier-transform infrared (DRIFTS) spectra were recorded on a Perkin-Elmer Paragon 1000PC spectrometer equipped with a MCT detector and a Spectra-Tech diffuse reflectance high temperature chamber with KBr windows allowing gases such as N_2 to flow through. Zeolites and catalysts (~40 mg) were ground into a fine powder with an agate mortar and transferred evenly into an aluminum sample cup. The samples were first dehydrated at 450°C for 1 h under flowing dry N_2 (treated with Supelco High Capacity Gas Purifier and OMI

[1] Author to whom correspondence should be addressed.

0021-9517/98 $25.00
Copyright © 1998 by Academic Press
All rights of reproduction in any form reserved.

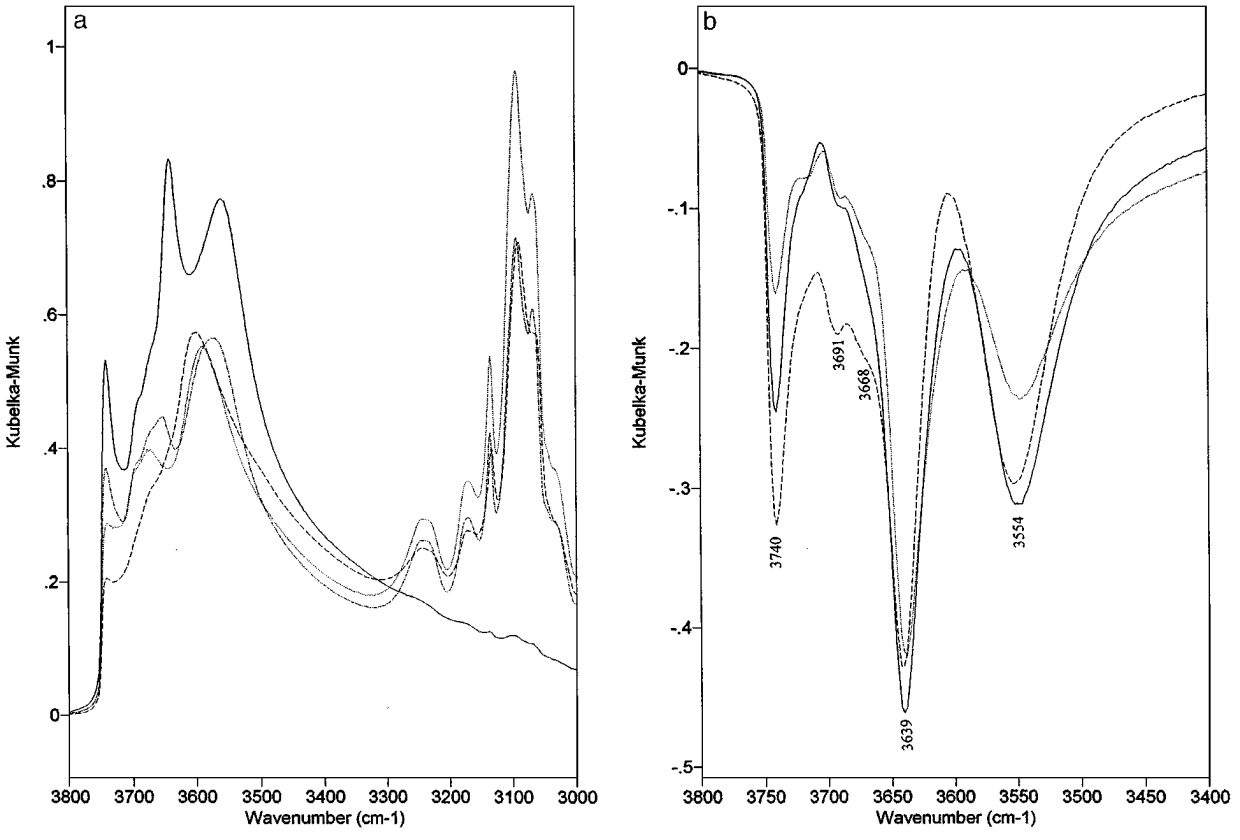

FIG. 1. (a) DRIFTS spectra of HY(LZ62) calcined in a shallow-bed fashion at 550°C for 4 h: (solid line) before pyridine adsorption; (dash line) pyridine adsorption at RT; (dotted line) pyridine adsorption followed by heating at 180°C for 1 h; (dash-dot-dot line) at 400°C for 1 h. All spectra were recorded at room temperature. (b) Difference spectra of the sample in (a), (solid line) after—before, (dash line) 180°C—before, and (dotted line) 400°C—before. (c) DRIFTS spectra of the same sample in spectral region 1700–1400 cm^{-1}. Labels are the same as in (a).

Indicating Purifier to remove H_2O and O_2 to less than 10 ppb) (40 ml/min), and then cooled to room temperature. Pyridine vapor (partial pressure, 18 mm Hg) was introduced in a N_2 stream for about one minute ($\sim 4 \times 10^{-5}$ moles of pyridine), then shut off. The system was equilibrated at room temperature for 1 h under flowing N_2, allowing removal of physisorbed pyridine. Samples were then heated to 180°C under flowing N_2 and maintained at this temperature for 1 h, then cooled to room temperature. Finally, the procedure was repeated at 400°C. Single beam spectra were collected at room temperature after heating using an automation program. For the single beam background spectrum, a fine ground KBr powder was used. The ratios of the sample spectra against the background spectrum were made, and the spectra were converted to Kubelka–Munk spectra (11) (defined by $(1 - \text{Transmittance})^2/(2 \times \text{Transmittance})$) after baseline and offset corrections. Difference spectra were obtained by subtracting the Kubelka–Munk sample spectra without pyridine from those containing pyridine. Due to interactions of adsorbed pyridine with the surface, bands generated by adsorption are positive, while bands "removed" by adsorption are negative.

Note that a flowing gas procedure is not as efficient as a vacuum. For similar levels of desorption, a higher temperature is needed.

Catalytic Activity Test

Cracking reactions were carried out at 487°C in a microactivity test unit using mid-continent gas oil with molecular average weight 264 and a final boiling point of 539°C. The reaction procedure was similar to that described by ASTM method 3907. A catalyst charge of 6 g was loaded in the reactor and pretreated at 487°C in flowing N_2 for at least 0.5 h. The catalyst/oil weight ratio was 5 and the oil delivery time was 48 s. The conversion was defined as the sum of the yields of gas, coke, and gasoline. Gasoline yields were obtained via simulation distillation chromatography. The activity is described by (grams of oil $\times$ %conversion)/(grams of catalyst $\times$ oil delivery time (s)).

RESULTS AND DISCUSSION

To answer the questions we posed, first we examined the shallow-bed and deep-bed calcined zeolites, then the

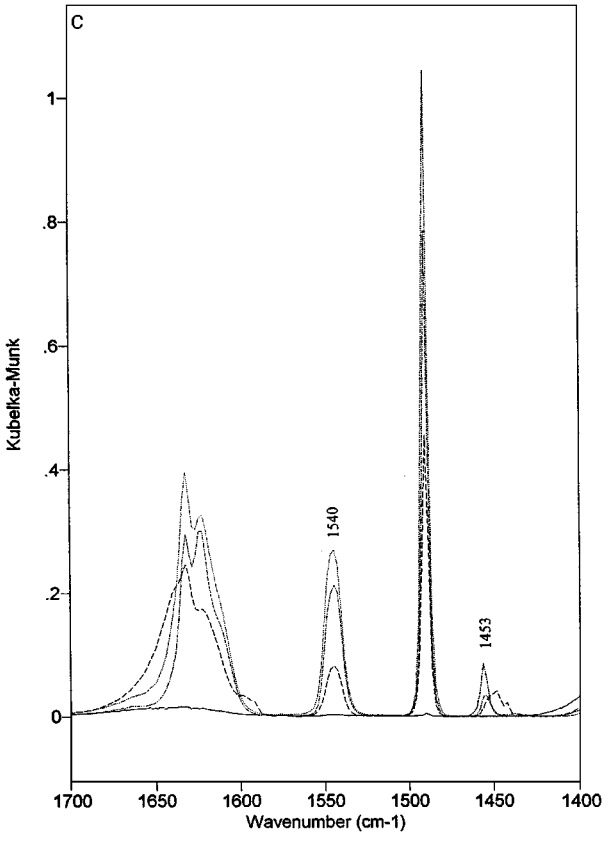

FIG. 1—*Continued*

steamed zeolites, and finally the steamed commercial FCC catalysts.

Shallow-Bed Calcined HY

Figure 1a shows DRIFTS spectra of shallow-bed calcined Y samples (LZ62) in the hydroxyl vibration region 3800–3000 cm^{-1}. The spectrum before pyridine adsorption has hydroxyl absorption bands at 3741, 3691, 3668, 3639, and 3554 cm^{-1} and the adsorbed pyridine bands appear around 3100 cm^{-1}. The 3741 cm^{-1} band is due to Si–OH groups, and the 3691 and 3668 cm^{-1} bands are due to Al–OH of nonframework Al species (12). Bands at 3639 and 3554 cm^{-1} are associated with bridged Al–OH–Si acidic hydroxyls located in supercages and hexagonal prisms, respectively. The presence of the bands at 3691 and 3668 cm^{-1} indicates that calcination under shallow-bed conditions causes framework dealumination. Upon pyridine adsorption, the intensities of all OH bands decrease, reflecting interactions of pyridine with hydroxyls (see Fig. 1a, dash-line spectrum). The remaining bands are broad and centered around 3740 and 3600 cm^{-1}. The nature of these bands is not exactly known, except for the 3740 cm^{-1} band which is due to Si–OH groups. The broad bands are more likely to be due to hydrogen-bonded species, inaccessible to pyridine molecules.

The type of hydroxyls interacting with pyridine can be differentiated more clearly by difference spectra (see Fig. 1b). First, it is clear from these spectra that all types of hydroxyls are disturbed by adsorbed pyridine. More significantly, Si–OH hydroxyls in the spectra and their survival after heat treatment (see Fig. 1b) suggest that these Si–OH groups are adjacent to acid sites (most likely Lewis acid sites) and are interacting with adsorbed pyridine. Otherwise, Si–OH groups should not be seen owing to their weak acidic nature. Furthermore, this feature depends on sample treatment. It is more substantial for shallow-bed calcined zeolites than for deep-bed calcined or steamed zeolites (see below).

This phenomenon was not addressed before in the literature, probably because of the very weak acidic nature of Si–OH. However, simultaneous interactions of adsorbed pyridine with both Lewis acid sites and their adjacent Si–OH groups reveals some details about the environment of these Lewis acid sites and configurations of the adsorbed pyridine molecules on the surface. Very recently, we have found (13) that Lewis acid sites on the surface of γ-alumina are surrounded by hydroxyls and that a specific arrangement of Lewis acid sites and hydroxyls is present. The disturbance of Si–OH by the adsorbed pyridine on Lewis acid sites may also reflect a similar situation occurring in the zeolite systems that Lewis acid sites have Si–OH groups as neighbors. Further studies are obviously needed to clarify this. The weak acidic nature of nonframework Al–OH and Si–OH–Al in the hexagonal prisms revealed by heat treatment experiments shown in Fig. 1b is consistent with that reported in the literature (8).

Figure 1c shows DRIFTS spectra of the same sample in the spectral region 1700–1400 cm^{-1}. The spectra are similar to those reported in the literature (8), showing the various adsorbed pyridine species: pyridine adsorbed on the Brönsted acid sites (~1540 cm^{-1}), those adsorbed on the Lewis acid sites (~1450 cm^{-1}), and hydrogen-bonded pyridine (~1585 cm^{-1}). The fact that there are no hydrogen bonded pyridine bands after heat treatment at 180° and 400°C supports the picture given above that Si–OH groups interacting with adsorbed pyridine are adjacent to Lewis acid sites. Another phenomenon observed in Fig. 1c is an increase of band intensity of pyridinium ions at ~1540 cm^{-1} after heating at 180°C. This phenomenon suggests that some pyridinium ions may form via a thermal activation process as observed by Ben Taarit *et al.* (14) on Cu–Y zeolites. However, space restrictions on pyridine diffusion in dealuminated zeolites may also play a role. Redistribution of adsorbed pyridine on Mg–Y zeolite upon heating has been reported (15).

Deep-Bed Calcined HY

Figure 2 shows DRIFTS spectra of 550°C-deep-bed-calcined HY and those after pyridine adsorption at room temperature followed by thermal treatment at 180

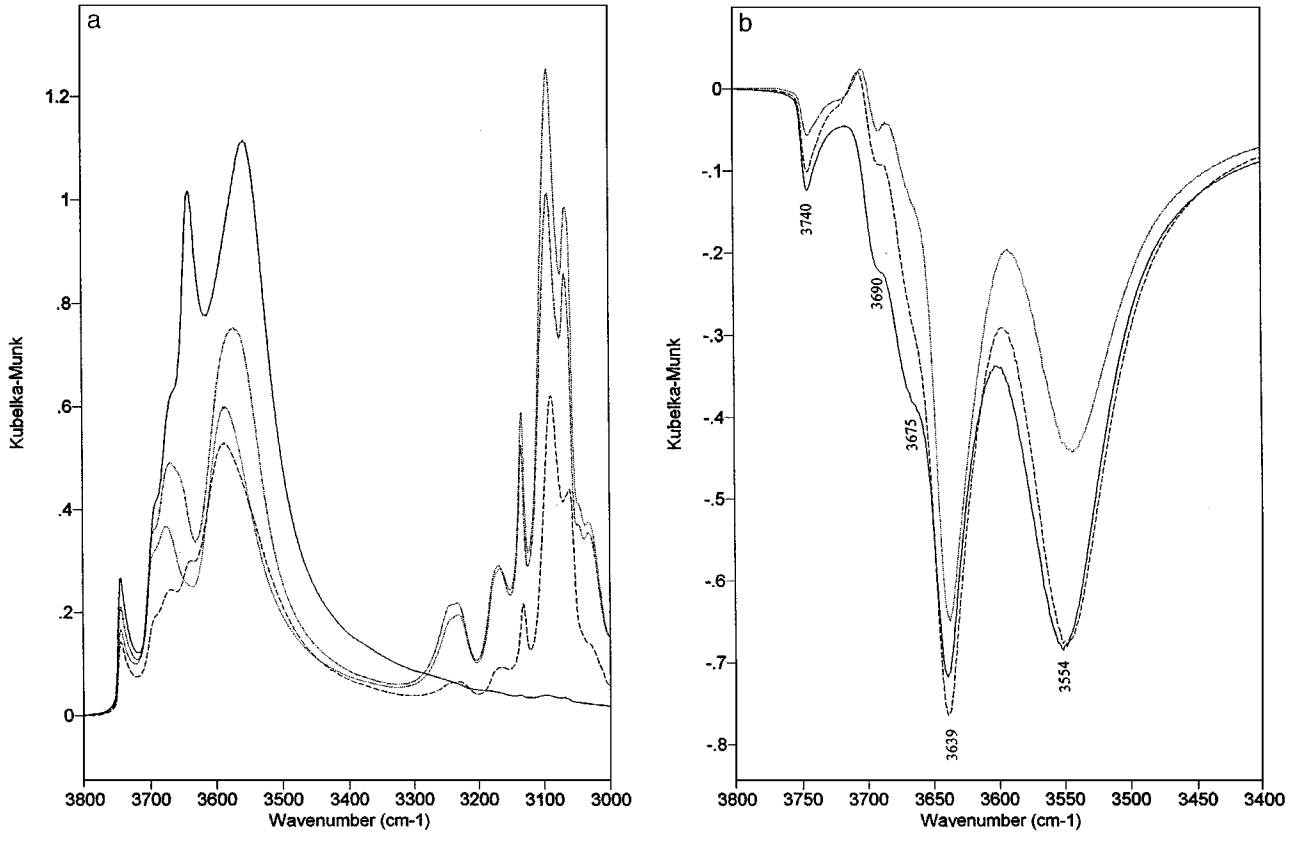

FIG. 2. (a) DRIFTS spectra of 550°C-deep-bed-calcined HY. (solid line) before pyridine adsorption; (dash line) pyridine adsorption at RT; (dotted line) pyridine adsorption followed by heating at 180°C for 1 h; (dash-dot-dot line) at 400°C for 1 h. All spectra were recorded at room temperature. (b) Difference spectra of the sample in (a), (solid line) after—before, (dash line) 180°C—before, and (dotted line) 400°C—before.

and 400°C. Three differences between the shallow and deep-bed calcined samples are observed: (1) More nonframework Al–OH groups are generated under deep-bed calcination (see the bands at 3690 and 3675 cm^{-1} in Figs. 2a and 2b). This is consistent with the general understanding that deep-bed calcination leads to more severe framework dealumination, compared to shallow-bed calcination. (2) The process generates fewer Si–OH groups (compare the band around 3740 cm^{-1} in Figs. 1b and 2b). This suggests that a deep-bed calcination causes, to some extent, "healing" of the Si–OH defect sites. (3) The relative intensity of Si–OH–Al in the hexagonal prisms is increased. The increase implies that more hexagonal prism OH groups after deep-bed calcination are available to pyridine. A strong dependence of interactions of hexagonal prism hydroxyls with pyridine on the framework Al composition has been found very recently by Echoufi and Gelin (16). With increasing framework Si/Al ratio, more hexagonal prism OH groups can be sensed by pyridine.

Steamed HY

Figure 3a shows DRIFTS spectra of steamed HY and those after pyridine adsorption at room temperature, followed by thermal treatment at 180 and 400°C. The difference spectra are given in Fig. 3b. Before pyridine adsorption, the hydroxyl region exhibits bands at 3744, 3735, 3692, 3669, 3660, 3628, 3596, 3563, and 3532 cm^{-1}. In comparison with shallow and deep-bed calcined samples, it is obvious that steaming generates more species and changes the surface. Bands at 3660, 3596, and 3532 cm^{-1} are new and not observed in the calcined samples. Si–OH groups around 3740 cm^{-1} are not intense, indicating the same healing process for the defect sites during steaming as seen in deep-bed calcination. The bands at 3692, 3669, and 3654 cm^{-1}, due to nonframework Al–OH, are weak compared to those of the deep-bed calcined sample, implying formation of alumina-like materials in the zeolite (17).

In addition to the same Al species with bands at 3692 and 3669 cm^{-1} as seen in the calcined samples, the 3654 cm^{-1} band represents a new type of nonframework Al species in the steamed sample. The new species is more acidic than the others, as evidenced by its different temperature response. The 3654 cm^{-1} band is recovered only after 400°C heat treatment (see Figs. 3b and 3c). The 3628 cm^{-1} band, due to bridged Si–OH–Al in supercages, and that at 3563 cm^{-1}, due to bridged Si–OH–Al in hexagonal prisms, are shifted

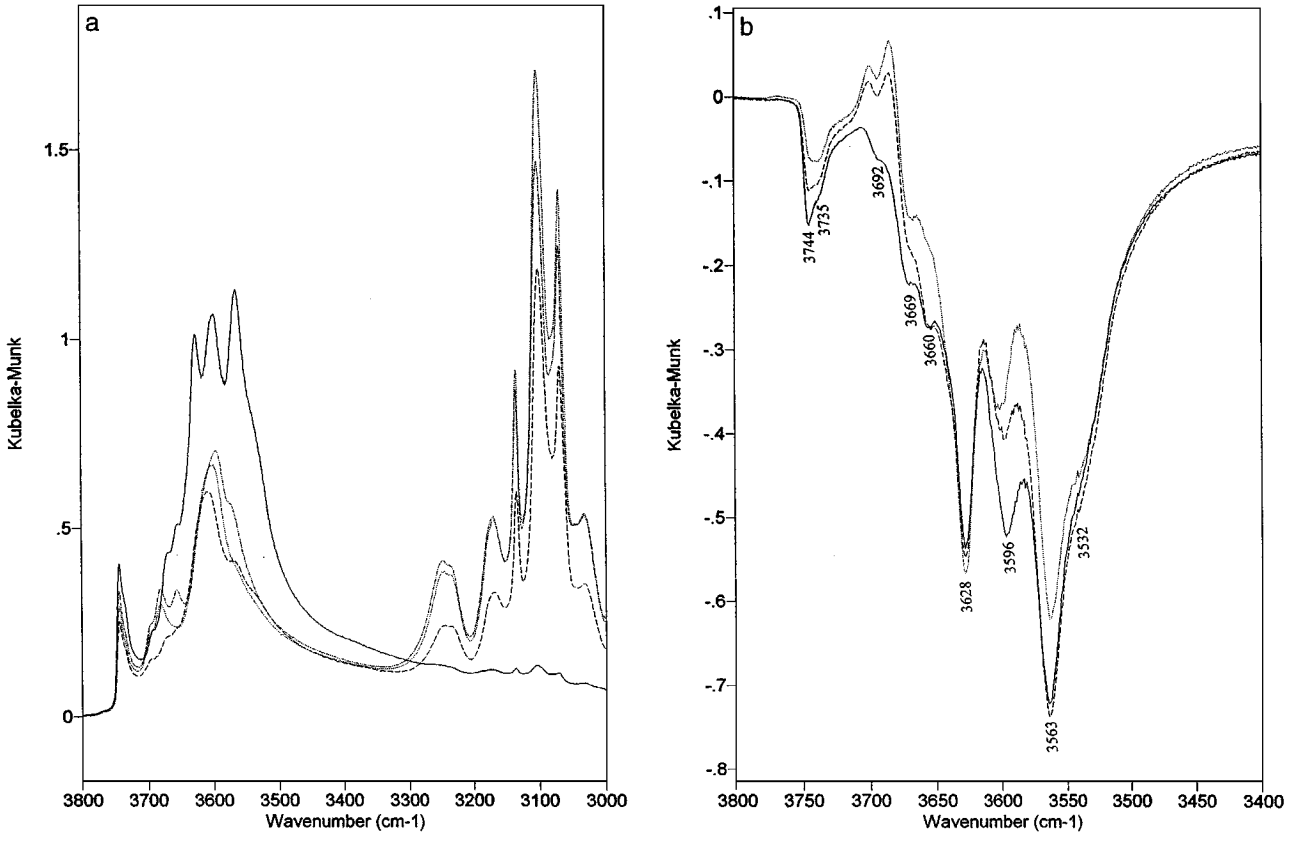

FIG. 3. (a) DRIFTS spectra of steamed HY. (solid line) before pyridine adsorption; (dash line) pyridine adsorption at RT; (dotted line) pyridine adsorption followed by heating at 180°C for 1 h; (dash-dot-dot line) at 400°C for 1 h. All spectra were recorded at room temperature. (b) Difference spectra of the sample in (a), (solid line) after—before, (dash line) 180°C—before, and (dotted line) 400°C—before. (c) Difference spectra of the sample in (a), (solid line) 180°C–RT, (dotted line) 400–180°C.

and narrowed compared with those in the calcined samples. The bathochromic shift of the 3639 cm^{-1} band to 3628 cm^{-1} indicates an increase in acid strength of this hydroxyl after steaming, which parallels the greater number of 0-Al NNN sites in the sample, while the hypochromic shift of the 3554 cm^{-1} band to 3563 cm^{-1} is due to weaker electrostatic interactions with surrounding framework oxygens owing to the decreased framework aluminum content.

The assignment for the 3596 cm^{-1} band is controversial (4, 18–22). It has been assigned, within certain variation of wavenumbers from 3610 to 3595 cm^{-1}, to various species such as nonacidic lattice hydroxyls (18), nonframework Al(OH) species (19, 20), strong acidic amorphous silica-alumina (21, 22), and strong acidic framework Si–OH–Al coordinated by nonframework aluminum species (4). Results obtained in the present study do not match these previous assignments. We observed interactions of these OH groups with adsorbed pyridine but not their strong acidity nature. Our temperature experiments clearly show that the 3595 cm^{-1} band acidity is weaker than that of the 3563 cm^{-1} band (see Fig. 3c). It recovers at a lower temperature than that of 3563 cm^{-1}. This contradictory result suggests that, even though a similar band is observed in this region, the IR-measured species may not be the same for all samples prepared in various ways. Care, therefore, must be taken when making an assignment for this band. Different sample preparations may generate different species with similar spectral features.

The species seen as a shoulder at 3532 cm^{-1} is more acidic than that of the 3596 cm^{-1} species (compare the spectra after treatment at different temperatures in Figs. 3b and c). Desorption of pyridine at different temperatures did not affect this band very much.

Steamed FCC Catalysts

Steaming causes framework dealumination of the zeolite in FCC catalysts. In the present study, FCC catalysts were steamed at 775 and 815°C and monitored for 24 h. Compositional changes of the zeolite framework were measured via framework vibration shifts. Figure 4 shows the band shift of symmetric stretching vibrations of framework as a function of steaming time. It is known from Fig. 4 that zeolite structure changes are rapid at these temperatures, and after

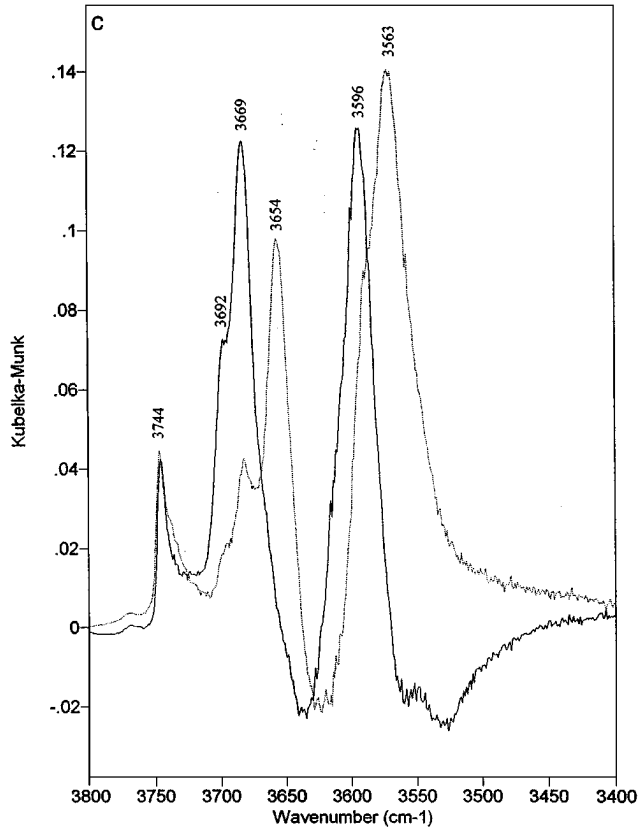

FIG. 3—*Continued*

approximately 5 h, the Si/Al ratio of the zeolite framework almost approaches a constant value.

Figure 5a shows DRIFTS spectra of FCC catalysts steamed at 815°C for 30 min and those after pyridine adsorption. The spectra show intense Si–OH bands around 3740 cm^{-1} and intense broad bands centered around 3550 cm^{-1}. After pyridine adsorption, a large proportion of the bands are not affected, particularly the broad one. Difference spectra given in Fig. 5b clearly show disturbance of the catalyst surface by adsorbed pyridine molecules. Hydroxyl groups interacting with pyridine are Si–OH (bands around 3740 cm^{-1}), bridged Si–OH–Al in supercages (band at 3629 cm^{-1}) and in hexagonal prisms (band at 3565 cm^{-1}), and a new species absorbing around 3522 cm^{-1}.

The observation of a very intense Si–OH band remaining after 180°C desorption supports the concept that some Si–OH groups are adjacent to Lewis acid sites. Nonframework Al–OH hydroxyl bands seen in the steamed zeolite Y are not observed for steamed FCC catalysts. This absence implies a rapid migration of the nonframework Al species either to the matrix or to form a separate amorphous phase during steaming. The new type of hydroxyl seen at 3522 cm^{-1} has been observed by several authors (23–25) for steamed and dealuminated zeolites Y and was assigned to framework OH groups coordinated by nonframework Al species (25). The literature assignment for this band (25) cannot be followed in the present study because our experiments show the species are not strong acidic sites, with no relationship to the species seen at 3596 cm^{-1} in the steamed zeolite (see Fig. 4b). Based on the features of this band (see below), we tentatively assign it to Si–OH–Al of an amorphous phase in the zeolite, generated by steaming. Temperature studies of the sample after pyridine adsorption reveal that the acidity of this hydroxyl is weaker than those in zeolite frameworks (see Fig. 5b).

Hydroxyl intensity changes are plotted versus steaming time in Fig. 6. Sites represented here are only those that can be reached by pyridine molecules. The assumption that pyridine-inaccessible hydroxyls do not contribute to catalytic activity should be reasonable for FCC catalysts. From the plots, two points are clear. First, the intensities of bridged hydroxyls both in the supercages and hexagonal prisms diminish differently with steaming. Hydroxyls in hexagonal prisms decrease faster than those in supercages. Steaming temperature also has effects. The higher the temperature, the more hydroxyls are destroyed. At 775°C, hexagonal prism hydroxyls survive 16 h, while at 815°C, they exist only for 4 h. The disappearance of this hydroxyl is not due to inaccessibility of pyridine, because it has been shown (16) that higher framework Si/Al ratio favors interactions of the small cage OH groups with pyridine. We therefore conclude that the hydroxyls in supercages are more stable towards steaming than those in hexagonal prisms. The difference in stability of these two types of hydroxyls is even more significant when high steaming temperatures were employed (compare Figs. 6a and b).

Second, new acid sites with a band at 3522 cm^{-1} are being produced during steaming. The band first becomes

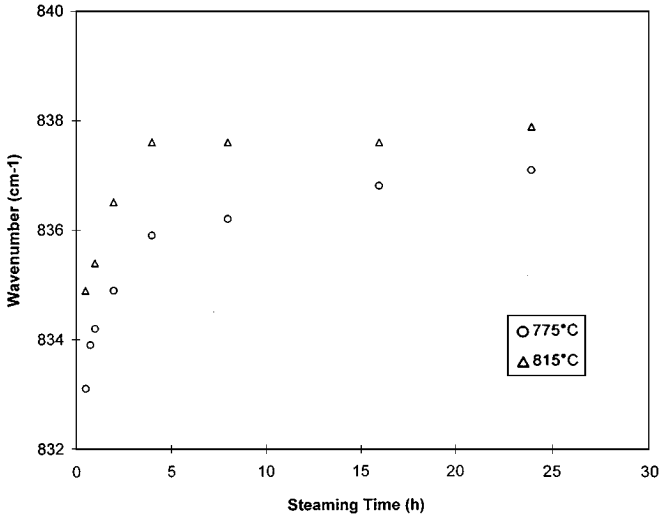

FIG. 4. Plot of band position of symmetric stretching vibration of zeolite framework as a function of steaming time.

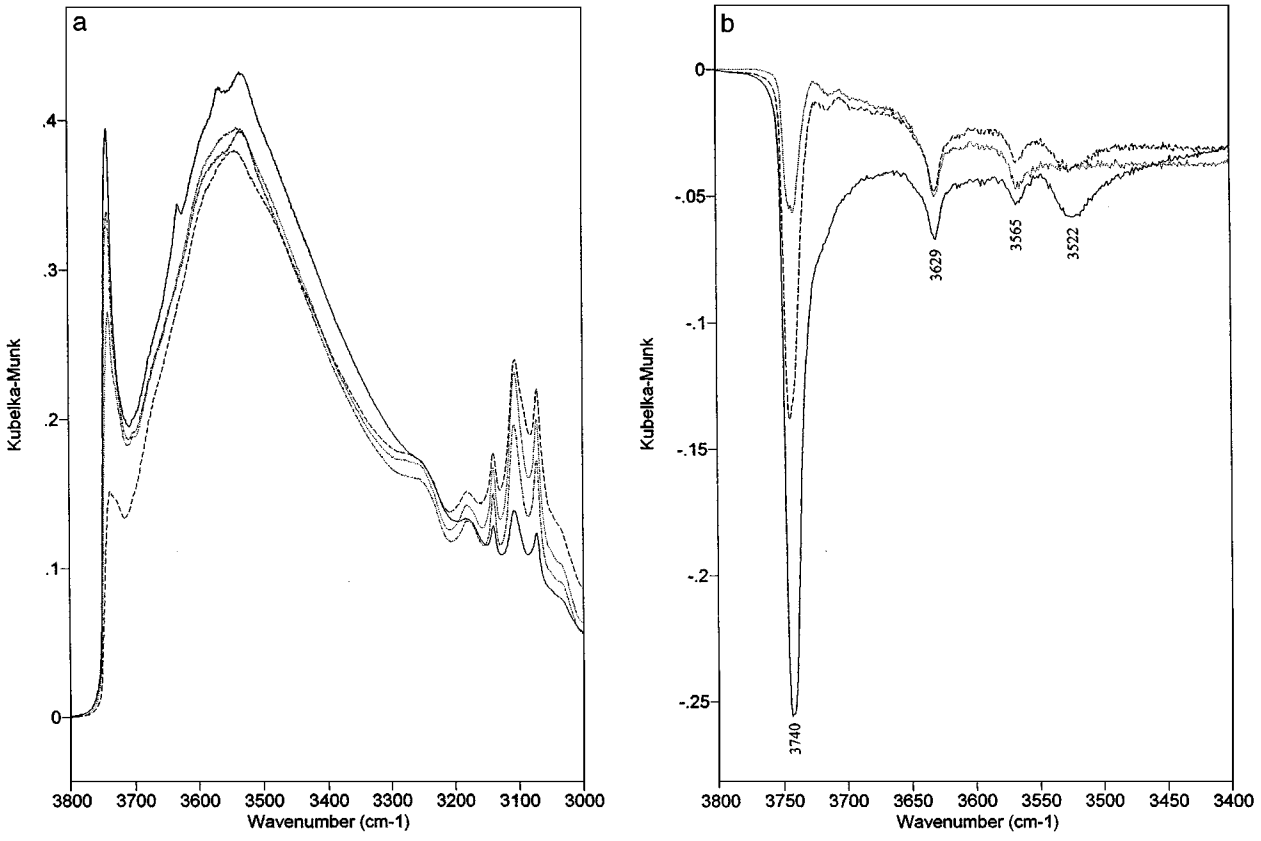

FIG. 5. (a) DRIFTS spectra of 815°C-steamed FCC catalysts. (solid line) before pyridine adsorption; (dash line) pyridine adsorption at RT; (dotted line) pyridine adsorption followed by heating at 180°C for 1 h; (dash-dot-dot line) at 400°C for 1 h. All spectra were recorded at room temperature. (b) Difference spectra of the sample in (a), (solid line) after—before, (dash line) 180°C—before, and (dotted line) 400°C—before.

intense with steaming, then decreases, passing through a maximum. The higher the temperature, the faster the maximum is reached. At 775°C, it needs ~8 h, while at 815°C, it requires only ~4 h. At later stages of steaming, the newly formed acid sites remain only as Brönsted acid sites (see Fig. 6).

In a recent study, Chen *et al.* (5) have observed a decrease in acid strength of FCC catalysts after extended steaming. Their observation apparently contradicts the common knowledge about zeolite acidity change upon steaming; acid strength increases with the increased number of isolated Al sites and does not change after the isolated Al sites become the only acidic sites. The present study resolves this dilemma. Steaming removes the original acid sites and produces a new type of Brönsted acid site with a lower acid strength. The new acid site dominates Brönsted acidity of the steamed catalyst after a certain period of steaming time. Activity of the later-stage steamed FCC catalysts, then, originates mainly from the newly generated Brönsted acid sites, not from the original Brönsted acid sites in the zeolite framework (see below).

Figure 7a shows the acidity changes as a function of steaming time at 775°C and 815°C. The measured Brönsted acidity using pyridine involves all types of acidic hydroxyls, as exemplified by the pyridinium ion band at ~1540 cm^{-1}, and exhibits a monotonic decrease with steaming time. Referring to Fig. 6, it is clear that different acid sites at different stages of steaming contribute to a different extent to the cracking activity. Since acidity diminishes faster than activity in the early stages of steaming, not all acid sites contribute to catalytic activity. This understanding corroborates the concept established recently that only some specific sites, for example, the isolated Al sites, are catalytic centers (6). However, from the changes of the acidic hydroxyls with steaming (see Figs. 6a and b), it is obvious that the newly formed Bronsted acid sites are involved in catalytic reactions, particularly after the original framework hydroxyls have disappeared. The parallel change of the acidity and the catalytic activity at the later stage of steaming demonstrates that the newly generated Brönsted acid sites are responsible for the ultimate activity.

Figure 7b shows changes of Lewis acidity during steaming at 775 and 815°C. Lewis acidity is also complicated by the changes of structure in the zeolites. The Lewis acidity quickly decreases within 2 h and then increases and decreases again, passing through a maximum at 4 h for

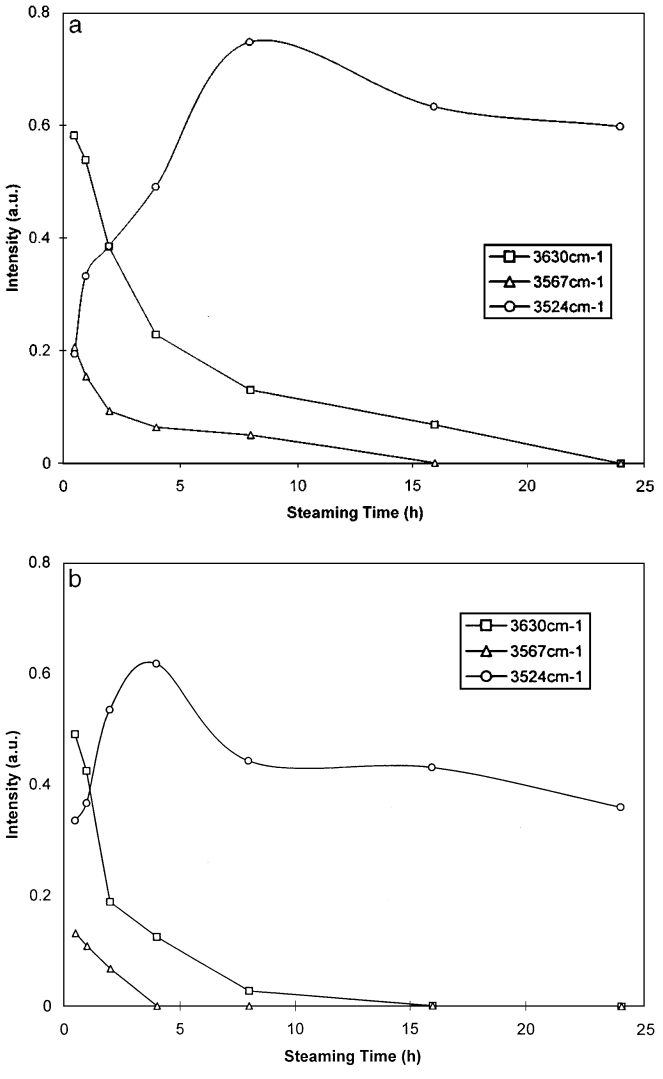

FIG. 6. (a) Intensity changes of hydroxyls of FCC catalyst upon steaming at 775°C. (b) Intensity changes of hydroxyls of FCC catalyst upon steaming at 815°C.

both temperatures. Since the pyridine adsorption method does not differentiate different Lewis acid sites, all we can say about Lewis acidity is that the sample experiences a generation and transformation of newly formed Lewis acid sites during steaming.

CONCLUSIONS

Studies of calcined and steamed zeolites and FCC catalysts using the pyridine adsorption-DRIFTS technique have demonstrated that some pyridine adsorbed on acid sites, probably Lewis acid sites, interact with adjacent Si–OH groups. The amount of the adjacent Si–OH depends on sample treatment conditions. Steaming zeolites and FCC catalysts generate a new type of Brönsted acid sites which are weaker in acid strength compared to those originally present in the zeolites. These acid sites contribute to the cracking activity of FCC catalysts, particularly after the samples are extensively steamed. During steaming, acidic hydroxyls in supercages survive longer than those in hexagonal prisms. Compared to the total acidity monitored by $\sim$1540 cm^{-1} with cracking activity, it is clear that for samples with short steaming time, not all acidity contributes to cracking activity. As steaming goes on, cracking activity tracks more than one type of acidic hydroxyls. Newly formed Brönsted acidic sites with a band at 3522 cm^{-1} contribute proportionally more to activity with increasing steam treatment. Eventually they dominate the catalytic cracking reactions.

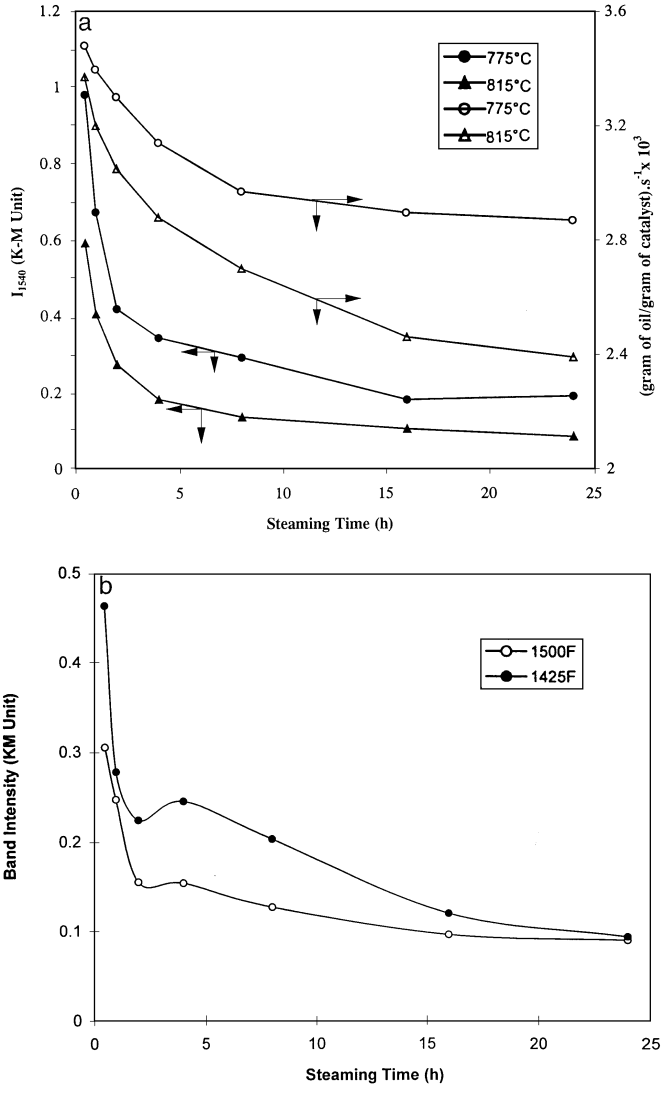

FIG. 7. (a) Changes of Brönsted acidity (described by the pyridinium band intensity at $\sim$1540 cm^{-1}) and activity (defined as (grams of oil $*$ %conversion)/(grams of catalyst $*$ oil delivery time (second)) of FCC catalyst upon steaming at 775 and 815°C. (b) Changes of Lewis acidity (described by the pyridine band intensity at $\sim$1450 cm^{-1}) of FCC catalyst upon steaming at 775 and 815°C.

ACKNOWLEDGMENTS

The authors thank Dr. D. Harris for providing the steamed HY sample and Robin Huff for preparation of the FCC catalysts. Drs. G. Walterman and R. J. Madon are thanked for their useful discussions.

REFERENCES

1. McDaniel, C. V., and Maher, P. K., *in* "Zeolite Chemistry and Catalysis" (J. A. Rabo, Ed.), p. 285. Amer. Chem. Soc., Washington, DC, 1976.
2. Auroux, A., and Ben Taarit, Y., *Therm. Acta.* **122**, 63 (1987).
3. Barthomeuf, D., *Mater. Chem. Phys.* **17**, 49 (1987).
4. Fritz, P. O., and Lunsford, J. H., *J. Catal.* **118**, 85 (1989).
5. Chen, D., Sharma, S., Cardona-Martinez, N., Dumesic, J. A., Bell, V. A., Hodge,G. D., and Madon, R. J., *J. Catal.* **136**, 392 (1992).
6. Ino, T., and Al-Khattaf, S., *Appl. Catal. A: General* **142**, 5 (1996).
7. Parry, E. P., *J. Catal.* **2**, 317 (1963).
8. Ward, J. W., *in* "Zeolite Chemistry and Catalysis" (J. A. Rabo, Ed.), p. 118 and references therein. Amer. Chem. Soc., Washington, DC, 1976.
9. McDaniel, C. V., and Maher, P. K., *in* "Molecular Sieves," p. 186. Soc. Chem. Ind., London, 1968.
10a. Haden, W. L., and Dzierzanowski, F. J., U.S. Patent 3,506,594 (1970).
10b. Haden, W. L., and Dzierzanowski, F. J., U.S. Patent 3,647,718 (1972).
11. "Bio-Rad Win-IR Reference Manual 091-0758A," p. 252.
12. Valyon, J., and Meszaros-Kis, A., *in* "Zeolites: Facts, Figures, Future" (P. A. Jacobs and R. A. van Santen, Eds.), p. 1015 and references therein. Elsevier Science, Amsterdam, 1989.
13. Liu, X., and Truitt, R. E.,*J. Am. Chem. Soc.* **119**, 9856 (1997).
14. Ben Taarit, Y., Primet, M., and Naccache, C., *J. Chim. Phys. Physicochim. Biol.* **67**, 1434 (1970).
15. Liengme, B. V., and Hall., W. K., *Trans. Faraday Soc.* **62**, 3229 (1966).
16. Echoufi, N., and Gelin, P., *Catal. Lett.* **40**, 249 (1996).
17. Shannon, R. D., Gardner, K. H., Staley, R. H., Bergeret, G., Gallezot, P., and Auroux, A. J., *J. Phys. Chem.* **89**, 4778 (1985).
18. Jacobs, P. A., and Uytterhoeven, J. B., *J. Chem. Soc. Faraday Trans. I* **2**, 373 (1973).
19. Anderson, M. A., and Klinowski, J., *Zeolites* **6**, 455 (1986).
20. Lohse, U., Loffler, E., Hunger, M., Stockner, J., and Patzelova, *Zeolites* **7**, 225 (1987).
21. Corma, A., Fornes, V., Perez-Pariente, J., Sastre, E., Martens, J. A., and Jacobs, P. A., *ACS Sump. Ser.* **368**, 555 (1988).
22. Garralon, G., Corma, A., and Fornes, V., *Zeolites* **9**, 84 (1989).
23. Khabtou, S., Chevreau, T., and Lavalley, J. C., *Microporous Materials* **3**, 133 (1994).
24. Chambellan, A., Chevreau, T., Khabtou, S., Marzin, M., and Lavalley, J. C., *Zeolites* **10**, 306 (1992).
25. Lonyi, F., and Lunsford, J. H., *J. Catal.* **136**, 566 (1992).